

Residual Chiral Symmetry Breaking in Domain-Wall Fermions

Chulwoo Jung,¹ Robert G. Edwards,² Xiangdong Ji,¹ and Valeriya Gadiyak¹

¹ *Department of Physics, University of Maryland, College Park, MD 20742, USA*

² *Jefferson Lab, 12000 Jefferson Avenue,*

MS 12H2, Newport News, VA 23606, USA

(Dated: DOE/ER/40762-210 July 2000)

Abstract

We study the effective quark mass induced by the finite separation of the domain walls in the domain-wall formulation of chiral fermion as the function of the size of the fifth dimension (L_s), the gauge coupling β and the physical volume V . We measure the mass by calculating the small eigenvalues of the hermitian domain-wall Dirac operator ($H_{\text{DWF}}(m_0)$) in the topologically-nontrivial quenched $SU(3)$ gauge configurations. We find that the induced quark mass is nearly independent of the physical volume, decays exponentially as a function of L_s , and has a strong dependence on the size of quantum fluctuations controlled by β . The effect of the choice of the lattice gluon action is also studied.

PACS numbers: 11.15.Ha, 12.38.G

Simulating massless or near-massless fermions on a lattice is a serious challenge in numerical quantum field theory. The origin of the difficulty can be traced to the well-known no-go theorem first shown by Nielsen and Ninomiya, which states that one can not write down a local, hermitian, and chirally-symmetric lattice fermion action without the fermion doubling problem [1]. Hence to have chirally-symmetric fermions on a lattice, one must use nonlocal actions in which the coupling between lattice sites do not identically vanish even when the separation becomes large. This implies that the lattice simulation with chiral fermions is necessarily more expensive than, e.g, the standard Wilson fermion in which only the nearest neighbor coupling is involved.

One of the lattice chiral fermion formalisms that have been studied extensively in recent years is the domain-wall fermion, first formulated by D. Kaplan [2] and later modified for realistic lattice simulation by Shamir [3]. In the domain-wall construction, one introduces an extra fifth dimension s with a finite extension. After discretization, the fifth direction has L_s number of lattice sites. If we put the same four-dimensional gauge configuration on every four-dimensional s slices, the five-dimensional massive theory admits a four-dimensional effective theory in which a left-handed chiral fermion lives near the $s = 0$ slice and a right-handed one near $s = L_s - 1$. Integrating out the heavy modes [4, 5, 6, 7], one obtains an effective four-dimensional chiral theory in the limit of $L_s \rightarrow \infty$.

For finite L_s , however, the two chiral modes can couple to produce an effective quark mass. Strong gauge field fluctuations can induce rather strong coupling, and hence rather large quark mass. This quark mass is expected to decrease exponentially as $L_s \rightarrow \infty$ with possible power law corrections. To gain a quantitative understanding of this induced mass, Columbia and other groups have considered several different ways to measure it. One way is to study the behavior of pion mass as the function of the wall separation L_s [8, 9]. The problem with this is that the pion mass may not vanish as $L_s \rightarrow \infty$ due to the finite volume effects, and hence the non-zero pion mass cannot be entirely attributed to the quark mass effect. Another way is to use the Gell-Mann–Oakes–Renner relation [10, 11]. However, this relation assumes a more complicated form in the domain-wall fermion formalism. The effective mass can be also measured by studying the anomalous contribution in the axial Ward–Takahashi(WT) identity [9, 12, 13].

In Ref. [14], we proposed to measure the induced effective quark mass by considering the eigenvalue of the hermitian domain-wall Dirac operator in the presence of the instanton background. In the $L_s \rightarrow \infty$ limit, the lattice version of the Atiyah-Singer theorem [15, 16] guarantees the existence of exact zero modes. For finite L_s , the lowest eigenvalues of the Dirac operator are not zero. We take the average of these would-be-zero eigenvalues as the effective quark mass. Our previous study for 150 gauge configurations at $\beta = 6.0$ yields an effective quark mass 0.0074 ± 0.0007 at $L_s = 8$, 0.0022 ± 0.0003 at $L_s = 12$, and 0.0008 ± 0.00013 at $L_s = 16$. The result is qualitatively consistent with those obtained from other methods [9, 12, 13].

In this paper, we report a more systematic study of the effective quark masses along this direction. In particular, we would like to understand the effects of different lattice sizes, the coupling constant β , and the form of gluon actions. Crucial to the size of the effective mass is the near-zero eigenvalues of the hermitian Wilson-Dirac operator at the fixed domain-wall height m_0 . These near-zero eigenvalues require large L_s to project out the correct effective Dirac operator. While we find that the effective mass is largely independent of the lattice size, it is a sensitive function of β and the form of gluon actions. For a strong coupling (small β) the effective low-energy theory is recovered only at very large L_s . We

find that the exponential decay rate for the effective mass is well described by the density of zero eigenvalues of the hermitian Wilson-Dirac operator. For an improved gluon action, the quantum fluctuations are strongly reduced and hence the domain-wall formalism works much more efficiently.

The domain-wall fermion was first introduced by D. Kaplan [2], based on an interesting observation that under certain conditions a five-dimensional massive fermionic theory has an effective four-dimensional massless fermion. For practical lattice simulations, Shamir considered a five-dimensional lattice having a finite extension in the fifth direction s ($s = 0, 1, \dots, L_s - 1$). The lattice domain-wall fermion action is a five-dimensional Wilson action at $r = 1$,

$$S_{\text{DWF}} = \sum \bar{\psi} D_{\text{DWF}}(m_0) \psi = - \sum_{x,s=0}^{L_s-1} \bar{\psi}_{x,s} \left[(m_0 - 5) \psi_{x,s} + P_R \psi_{x,s-1} + P_L \psi_{x,s+1} + \frac{1}{2} \sum_{\mu} \left((1 - \gamma_{\mu}) U_{x,\mu} \psi_{x+\mu,s} + (1 + \gamma_{\mu}) U_{x-\hat{\mu},\mu}^{\dagger} \psi_{x-\hat{\mu},s} \right) \right], \quad (1)$$

where m_0 is the negative of the conventional Wilson mass and $P_{R,L} = \frac{1}{2}(1 \pm \gamma_5)$ is the chiral projection operators. The physical significance of m_0 is the ‘‘height of the domain wall’’. Like the inverse of the lattice spacing $1/a$ (taken to be 1), it acts as a heavy mass scale of the theory. The gauge fields live on the four-dimensional sub-lattices and are independent of s . Dirichlet boundary conditions are applied to the fermion fields at $s = -1$ and L_s . For the sake of simplicity, we omit the Pauli-Villars fields which can be introduced to cancel the bulk of the heavy modes of the theory. The interested reader can consult Ref. [3] for details.

As shown in Ref. [3], the above construction in the absence of gauge fields has a low-energy effective theory with two massless chiral fermions near $s = 0$ and $L_s - 1$ in the limit of $L_s \rightarrow \infty$. Thus, a single-flavor massless Dirac field $q(x)$ can be constructed from the domain-wall fermion field $\psi(x, s)$ as

$$q(x) = P_L \psi(x, s = 0) + P_R \psi(x, s = L_s - 1). \quad (2)$$

An explicit fermion mass, m_f , for the chiral modes can be introduced through the modified boundary conditions,

$$P_L \psi_{x,L_s} = -m_f P_L \psi_{x,0}, \quad P_R \psi_{x,-1} = -m_f P_R \psi_{x,L_s-1}. \quad (3)$$

Substituting this into Eq. (1), we obtain a generic fermion mass term.

To study the low-energy aspects of the domain-wall fermion action, we introduce the hermitian domain-wall Dirac operator, $H_{\text{DWF}}(m_0) = R_s \gamma_5 D_{\text{DWF}}(m_0)$, where R_s denotes the reflection in the fifth direction. Because of the low-energy property mentioned above, we expect that the low-lying spectrum of $H_{\text{DWF}}(m_0)$ resembles that of a massless Dirac particle and contributes dominantly to low-energy physical observables. [Unlike the four-dimensional Wilson-Dirac operator $D_{\text{W}}(m_0)$ which has a simple hermitian-conjugation property, we find that the domain-wall Dirac operator $D_{\text{DWF}}(m_0)$ has a peculiar spectrum with obscure physical significance.]

A more direct way of studying the low-energy physics of the domain-wall fermion is to integrate out all heavy modes. This has been done by a number of authors [4, 5, 6, 7]. The result has a very simple form

$$S^{\text{eff}} = \sum_{x,y} \bar{q}(x) D_{L_s}^{\text{eff}}(a_5, m_0) q(y), \quad (4)$$

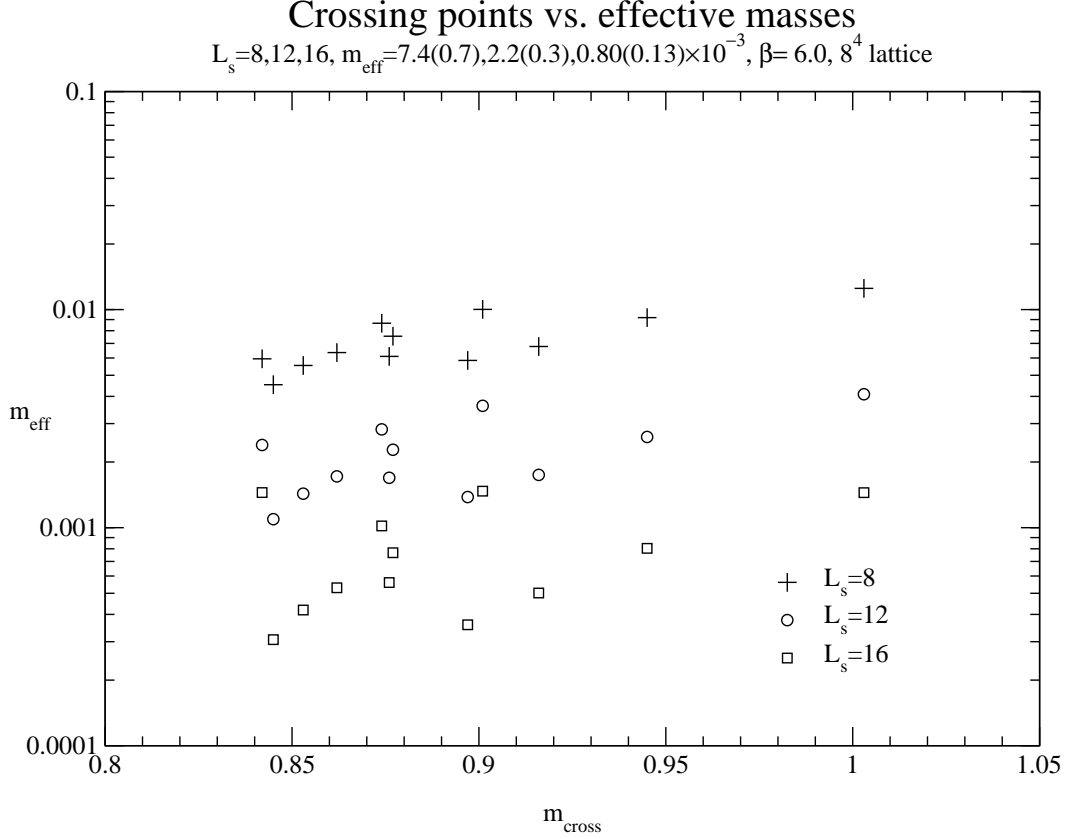


FIG. 1: Effective quark mass induced by domain walls for the Monte Carlo configurations at $\beta = 6.0, 8^4$ lattice. L_s is the number of lattice sites in the fifth direction.

where we have made the lattice spacing in the fifth direction a_5 explicit and [7]

$$D_{L_s}^{\text{eff}}(a_5, m_0) = \frac{1 + \gamma_5 \tanh\left(\frac{L_s}{2} H(a_5, m_0)\right)}{1 - \gamma_5 \tanh\left(\frac{L_s}{2} H(a_5, m_0)\right)},$$

$$H(a_5, m_0) = \frac{1}{a_5} \ln\left(\frac{1 + a_5 P_R H_W(m_0)}{1 - a_5 P_L H_W(m_0)}\right). \quad (5)$$

$H_W(m_0) = \gamma_5 D_W(m_0)$ is the hermitian Wilson-Dirac operator. The four-dimensional effective Dirac operator $D_{L_s}^{\text{eff}}(a_5, m_0)$ can be used to calculate the propagator of the chiral fermion modes. If an observable involves the fermion determinant, we must take into account the contribution from the Pauli-Villars particles as well. The effective Dirac operator in the fermion determinant is

$$\overline{D}_{L_s}(a_5, m_0) = \frac{1}{2} \left[1 + \gamma_5 \tanh\left(\frac{L_s}{2} H(a_5, m_0)\right) \right]. \quad (6)$$

In the limit of a continuous fifth dimension, i.e. $a_5 \rightarrow 0$, $H(a_5, m_0)$ in the above expression becomes

$$H(a_5 = 0, m_0) = H_W(m_0). \quad (7)$$

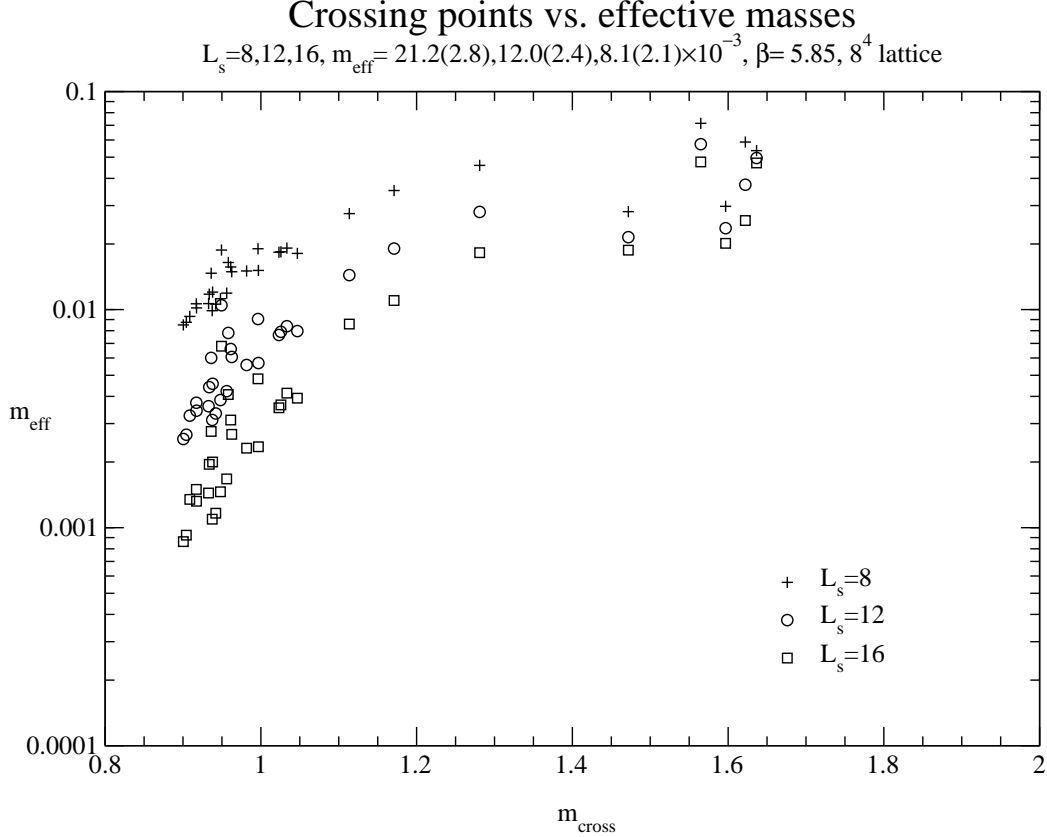


FIG. 2: Effective quark mass induced by domain walls for the Monte Carlo configurations at $\beta = 5.85, 8^4$ lattice. L_s is the number of lattice sites in the fifth direction.

And if we take the limit $L_s \rightarrow \infty$ as well,

$$\tanh\left(\frac{L_s}{2}H\right) \rightarrow \epsilon(H) = \theta(H) - \theta(-H) , \quad (8)$$

the Dirac operator $\overline{D}_\infty(a_5 = 0, m_0)$ becomes the well-known Neuberger overlap operator [4]. On the other hand, if we take $L_s \rightarrow \infty$ first, we have

$$\overline{D}_\infty(a_5, m_0) = \frac{1}{2} [1 + \gamma_5 \epsilon(H(a_5, m_0))] . \quad (9)$$

The difference from the Neuberger overlap operator [4] is that $H(a_5, m_0)$ is now a function of $H_W(m_0)$ (see Eq. (5)).

The above discussion leads to a simple and natural way of defining the topology of lattice gauge configurations [16]. The effective domain-wall Dirac operator at $L_s \rightarrow \infty$ ($\overline{D}_\infty(a_5, m_0)$) has the following interesting property. If the hermitian operator $H(a_5, m_0)$ has unequal numbers of positive and negative eigenvalues, its determinant vanishes; this means that $\overline{D}_\infty(a_5, m_0)$ has zero-energy eigenvalues. Inspired by the Atiyah-Singer theorem in the continuum spacetime, one can regard the appearance of the zero eigenvalues as the signal for a nontrivial topology of the lattice configuration. Since the number of positive and negative

levels are the same for $m_0 < 0$, the difference between the number of positive and negative levels at a positive m_0 can be calculated by tracking the spectral flow of all eigenvalues of $H(a_5, m)$ between $m = 0$ and $m = m_0$ and locating the level crossings [16, 17, 18]. The topological index of a gauge configuration is given by the difference of the number of positive and negative energy levels of $H(a_5, m_0)$. The effective domain-wall Dirac operator $\overline{D}_\infty(a_5, m_0)$ has the same number of zero eigenvalues as the topological index. Rather than find the eigenvalues of $H(a_5, m)$, a computationally simpler method can be used for $m < 2$ and $a_5 = 1$ where the spectral flow of the lowest eigenvalues of the hermitian Wilson-Dirac operator $H_W(m)$ are tracked between $m = 0$ and $m = m_0 < 2$. The topological index thus produced is the same as that of the effective domain-wall Dirac operator $\overline{D}_\infty(a_5, m_0)$ [7].

For finite L_s , however, the chiral modes of $\overline{D}_{L_s}(a_5, m_0)$ corresponding to the gauge field topology do not have exact zero eigenvalue. The limit is approached exponentially as $L_s \rightarrow \infty$. Since the low-lying eigenvalues of the effective Dirac operator $\overline{D}_{L_s}(a_5, m_0)$ must reproduce those of $H_{\text{DWF}}(m_0)$, the latter has the same number of exponentially-small eigenvalues as the topological index. We *define* the finite- L_s induced fermion mass m_{eff} as an average of these quasi-zero eigenvalues.

In a previous publication [14], we have calculated m_{eff} from 150 configurations on an 8^4 lattice at $\beta = 6.0$ and $m_0 = 1.8$. Here again we show m_{eff} for each of the zero modes in Fig. 1 where the horizontal axis is the Wilson mass m representing the locations of the level crossings in the eigenvalue flow of $H_W(m)$, and the vertical axis is m_{eff} . For those configurations with multi-level crossings, we relate m_{eff} and m by assuming that the spectrum flow is repulsive or levels do not cross, and this simplifies the presentation. The results for three different L_s are shown with three different symbols.

How does the effective mass change as the coupling grows stronger (smaller β)? To answer this question, we have generated 100 $SU(3)$ lattice gauge configurations on a lattice size 8^4 , 50 each at $\beta = 5.85$ and 5.7 . We measure the eigenvalue flow of the hermitian Wilson-Dirac operator, and calculate the eigenvalues of $H_{\text{DWF}}(m_0)$ corresponding to the nontrivial topology of the gauge configurations. For larger lattice spacing, quantum fluctuations are stronger, and some of these fluctuations can be misidentified as small size instantons. It turns out that they can induce strong couplings between the left- and right-handed chiral modes and are detrimental to the existence of the low-energy effective theory. Indeed, for the same L_s , the effective masses are much larger at the smaller β 's than those at $\beta = 6.0$. For example, with $L_s = 16$, m_{eff} is 0.0008 at $\beta = 6.0$, 0.008 at $\beta = 5.85$, and 0.018 at $\beta = 5.7$.

Moreover, for the same lattice size, physical volume is larger at smaller β , and hence can house more instantons. As shown in Fig. 2 for $\beta = 5.85$ and Fig. 3 for $\beta = 5.70$, the total number of instantons in the 50 configurations is now 32 and 96, respectively. The level crossings happen at larger m_0 compared with Fig. 1. For $\beta = 5.7$, there are several crossings very close to $m_0 = 1.8$. This is in contrast to what has been observed at $\beta = 6.0$, where the crossings occur mostly around $m = 1.0$ [14, 18]. The equal spacing between m_{eff} at different L_s is a clear signal for the exponential decay. However, there is a significant variation in the rate among all the crossings, as evident in the figures. (Note: After the analysis for the paper is completed, the recent work of the CP-PACS [12] and RBC [13] collaborations became available, which shows the signal for varying rate of exponential decay and/or nonvanishing effective mass in the $L_s \rightarrow \infty$ limit. This behavior is only seen at a much larger L_s than those studied here. However, it is interesting to note that averaging eigenvalues with varying exponential rate can easily reproduce the large L_s behavior of the

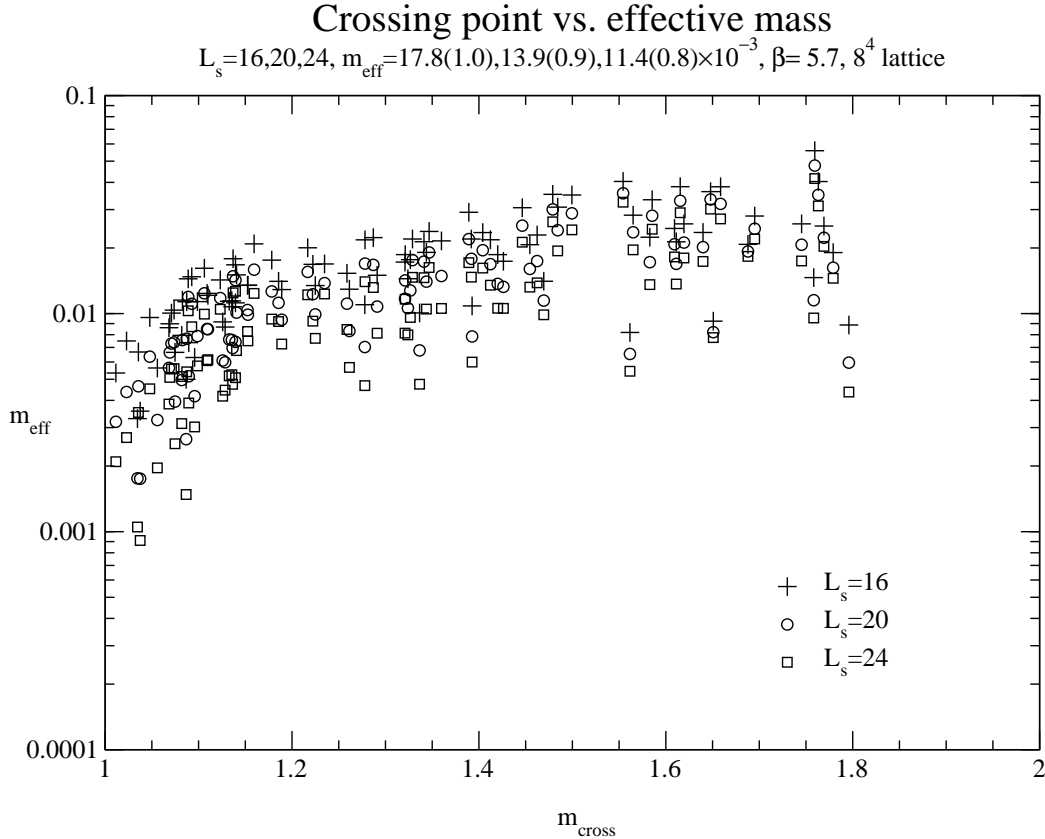


FIG. 3: Effective quark mass induced by domain walls for the Monte Carlo configurations at $\beta = 5.7, 8^4$ lattice. L_s is the number of lattice sites in the fifth direction.

effective mass observed in the aforementioned reference.)

To see the volume dependence at a fixed m_0 and β , we also measure the effective mass on a set of 50 configurations on an $8^3 \times 16$ lattice at $\beta = 5.85$. The total number of instantons is now 64, doubling that on the 8^4 lattice. We notice there are several crossings very close to $m_0 = 1.8$. The average effective mass turns out to be essentially the same as that on the smaller lattice. A similar conclusion can be drawn by comparing m_{eff} at $\beta = 6.0$ and $V = 8^4$ with that at the same β and $V = 16^3 \times 24$ in Ref. [9], although we note that the way of determining the effective mass there is quite different. This weak dependence on the size of the volume may allow us to extrapolate our quantitative results to large lattices necessary for realistic simulations.

We also measure the effective mass on a set of 200 configurations generated from the 1-loop Lüscher-Weisz gauge action [19] with the tadpole improvement. (Crossings from only 50 lattices are shown in Fig. 5.) Similar studies using various improved gauge actions, including an RG improved action [20] are reported in [11, 12]. The gauge coupling ($\beta = 7.9$) corresponds to a spacing of ~ 0.16 fm, similar to $\beta = 5.7$ of the Wilson action. The spectral flow and the domain-wall eigenvalues are studied with the same Wilson-Dirac operator. As shown in Fig. 5, the number of instantons as well as the distribution of the crossings differs significantly from the Wilson action at similar lattice spacing. Because of the decrease of small-scale quantum fluctuations, the probability of the crossing at $m_0 > 1.2$ is heavily

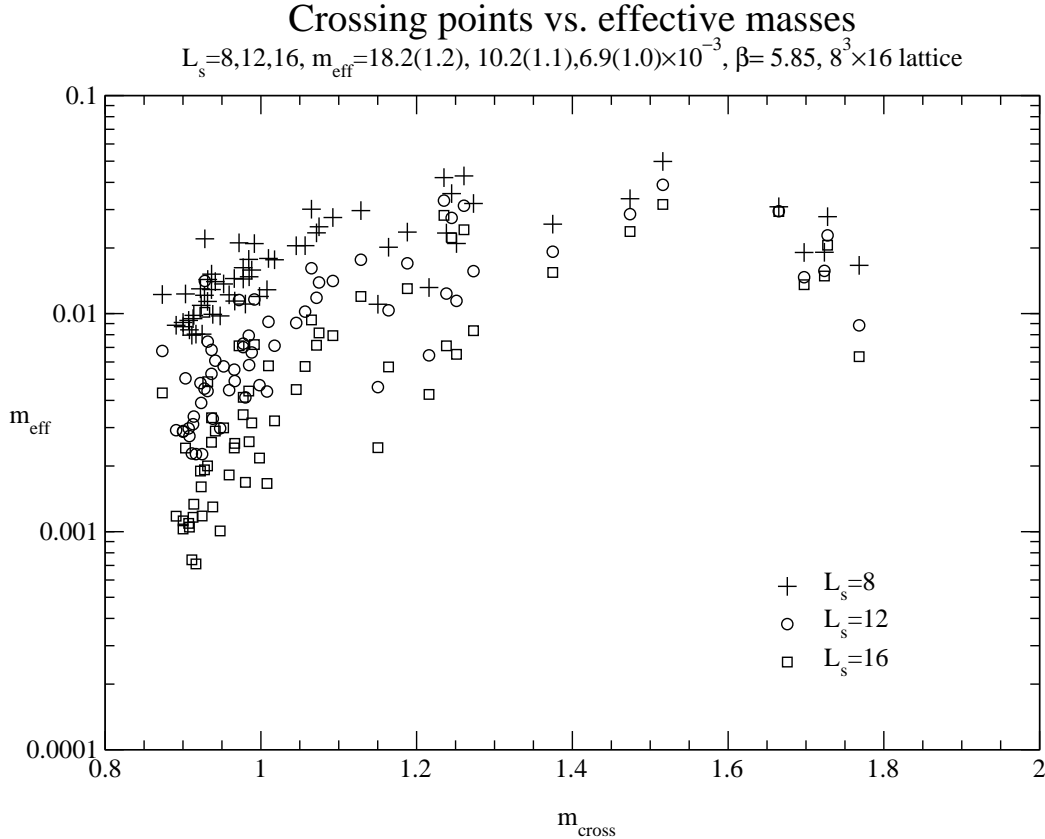


FIG. 4: Effective quark mass induced by domain walls for the Monte Carlo configurations at $\beta = 5.85$, $8^3 \times 16$ lattice. L_s is the number of lattice sites in the fifth direction.

suppressed, and the density of small eigenvalues of $H_W(m_0)$ is also much smaller ($\sim 2.7 \times 10^{-4}$, compared to $\sim 1.8 \times 10^{-3}$ for $\beta = 5.7$ Wilson action). Therefore, the effective mass decreases faster as a function of L_s . The average effective mass at $L_s = 16$ is $\sim 6 \times 10^{-3}$, compared to 18×10^{-3} from the Wilson action at $\beta = 5.7$.

The origin of the induced chiral fermion mass is the finiteness of L_s . More specifically, the hyperbolic-tangent function at finite L_s is used to approximate the ϵ function (Eq. (8)). This approximation is good for large eigenvalues of $H(a_5, m_0)$, but poor for small ones. For smaller β , $H(a_5, m_0)$ has more small eigenvalues and hence the hyperbolic-tangent is a worse approximation of the ϵ -function. This point is also reflected in the dependence of the exponential decay rate on the density of the zero eigenvalues of $H_W(m_0)$ ($\rho(0; m_0)$). We note that since the gauge fields are replicated along the fifth dimensional slices, the relevant length scale in the fifth dimension is the inverse of the rate of exponential decay (α) and by simple engineering dimensions is given qualitatively by the density of zero eigenvalues of $\rho(0; m_0)^{1/3}$. In Fig. 6, we have plotted $1/\alpha$ as a function of $\rho(0; m_0)$. The rate α for each coupling is calculated by fitting $m_{\text{eff}} = m_0 \exp[-\alpha L_s]$ at different L_s . The statistical errors are estimated by doing correlated fits to single-eliminated jackknife blocks. The inverse decay rates from all the configurations studied show an approximate linear scaling as $\rho(0; m_0)^{1/3}$. This suggests that the density of small eigenvalues is indeed the dominating factor for the exponential decay rate of domain-wall fermions.

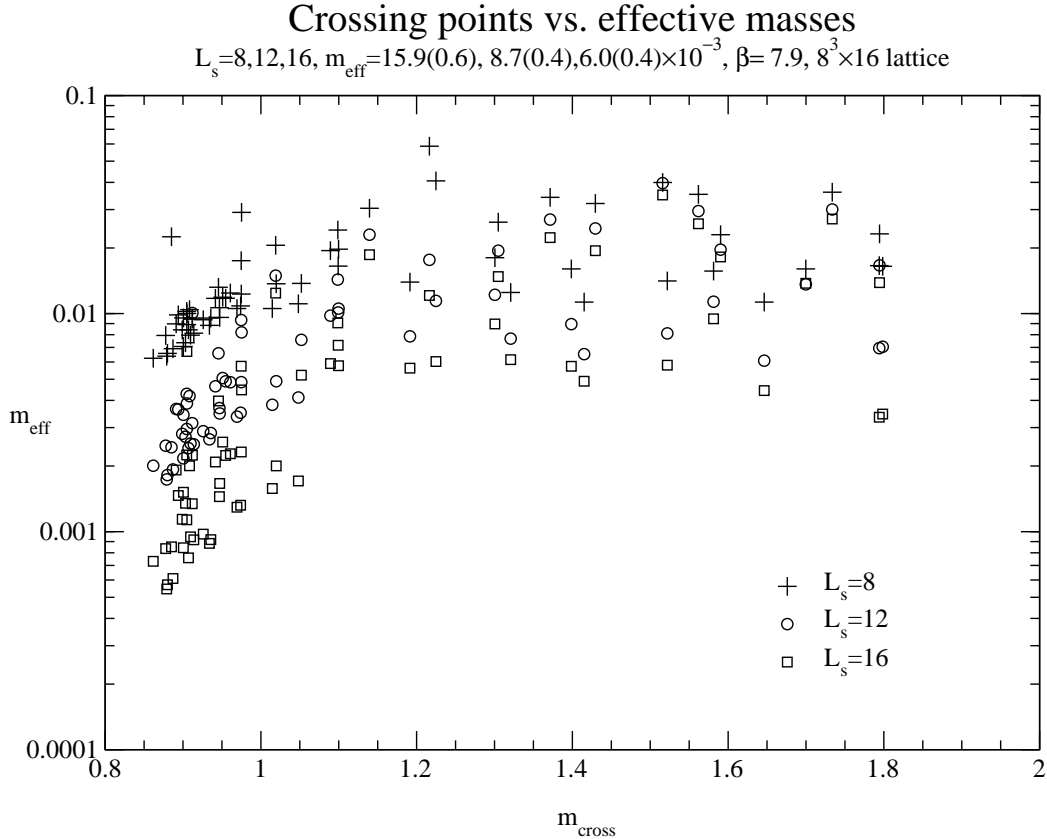


FIG. 5: Effective quark mass induced by domain walls for the 50 Monte Carlo configurations generated by the 1-loop, tadpole improved gauge action [19] on a $\beta = 7.9, 8^3 \times 16$ lattice. L_s is the number of lattice sites in the fifth direction.

Effective masses thus obtained for the different gauge coupling and L_s are plotted in Fig. 7. The data from Ref. [9, 10] are also included for comparison. For a given gauge coupling, different volumes and methods of measurements have little effect on the size of the effective mass as well as the rate of exponential decay. However, the change of gauge action affects the effective mass significantly. It is quite clear from the figure 7 that for a practical simulation of the domain-wall fermion, one either chooses a large β with the conventional Wilson action or an improved action keeping lattice spacing large.

To summarize, we have studied the residual chiral symmetry breaking present in domain-wall fermion by measuring the eigenvalues of the hermitian domain-wall Dirac operator corresponding to the topology of the lattice gauge configurations. Individual eigenvalues for the topological zero modes show clear exponential behavior in L_s . We regard these eigenvalues as the induced mass for the surface chiral modes at finite L_s separation.

For L_s and β , we see little variation of m_{eff} as a function of the volume. This is in some sense expected because the coupling of the chiral modes between the opposite walls has little to do with the size of the four-dimensional slice. On the other hand, a strong dependence on β is observed. In particular, the effective mass is much larger at $\beta = 5.85$ or 5.7 than that at $\beta = 6.0$. For the improved gauge action, the spurious fluctuations are reduced significantly and the L_s needed to obtain a good chiral symmetry is reduced. Since

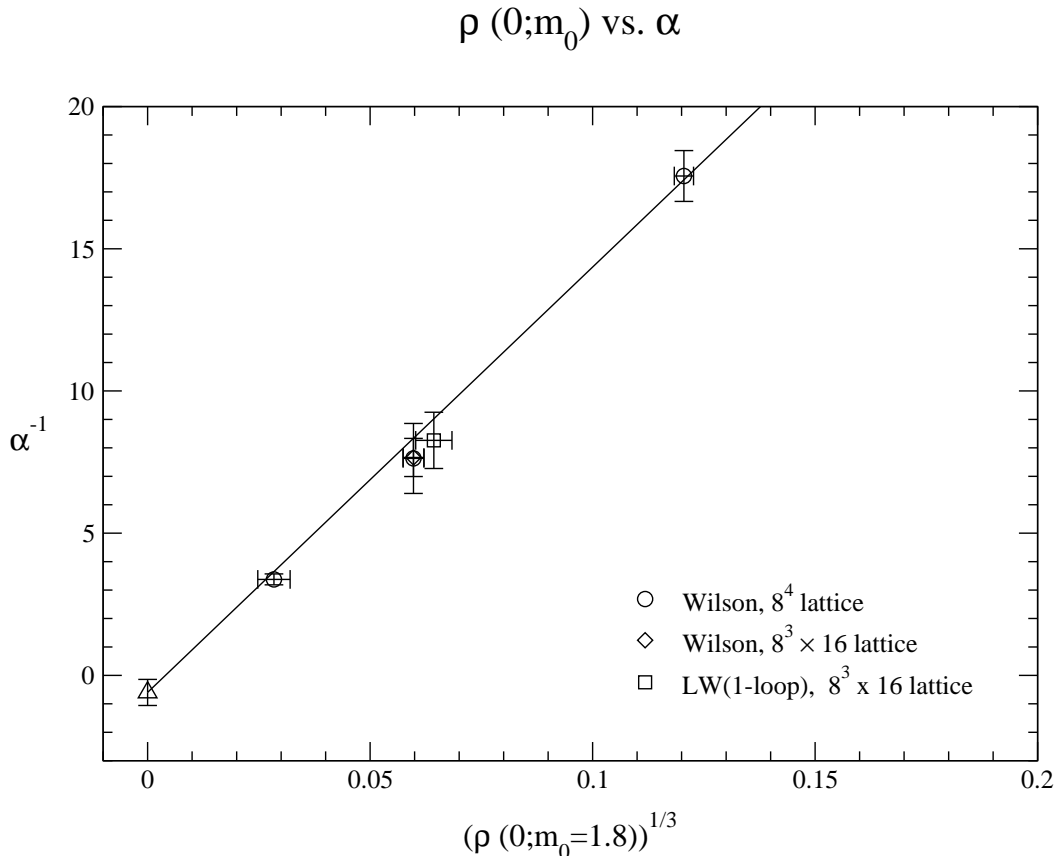


FIG. 6: Average coefficient of the exponential decreases as a function of $\rho(0; m_0)$. The extrapolation of the fit to the continuum limit for the Wilson gauge backgrounds is shown on the left. $\rho(0; m_0)$ for the Wilson and improved gauge action are from Ref. [18] for $8^3 \times 16$ lattices.

the additional computation needed for the improved action is negligible, using improved gluon actions may enable us to simulate domain-wall fermions with larger lattice spacing.

Acknowledgments

We thank N. Christ and J. Negele for useful discussions related to the subject of this paper. The numerical calculation reported here were performed on the Calico Alpha Linux Cluster and the QCDSF at the Jefferson Laboratory, Virginia. C.J., X.J. and V.G. are supported in part by funds provided by the U.S. Department of Energy (D.O.E.) under cooperative agreement DOE-FG02-93ER-40762. R.G.E. was supported by DOE contract DE-AC05-84ER40150 under which the Southeastern Universities Research Association (SURA) operates the Thomas Jefferson National Accelerator Facility (TJNAF).

-
- [1] H. B. Nielsen and M. Ninomiya, Nucl. Phys. **B185**, 20 (1981).
 [2] D. B. Kaplan, Phys. Lett. B **288**, 342 (1992).

Average effective masses

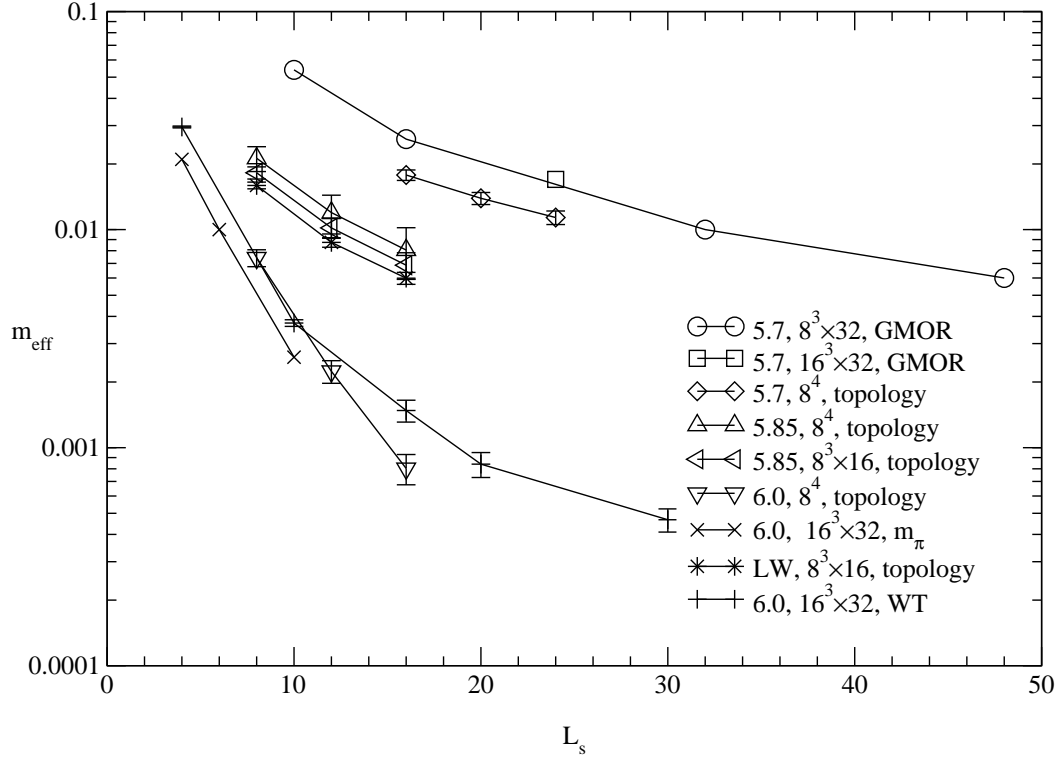


FIG. 7: Average effective masses from various observables as a function of L_s . Effective masses from $\beta = 5.7$, GMOR relation are from Ref. [10]. Data for $\beta = 6.0$, m_π and the axial WT identity are from Ref. [9] and [12], respectively. LW denotes the 1-loop, tadpole improved gauge action from Ref. [19].

- [3] Y. Shamir, Nucl. Phys. **B406**, 90 (1993);
Y. Shamir, Nucl. Phys. **B417**, 167 (1994);
V. Furman and Y. Shamir, Nucl. Phys. **B439**, 54 (1995).
- [4] H. Neuberger, Phys. Rev. D **57**, 5417 (1998).
- [5] Y. Kikukawa and T. Noguchi, hep-lat/9902022.
- [6] A. Boriçi, hep-lat/9909057..
- [7] R. G. Edwards, U. M. Heller, hep-lat/0005002
- [8] P. Chen et al., presented at 29th Intl. Conf. on High-Energy Physics (ICHEP 98), Vancouver, Canada, 23-29 Jul 1998. In **Vancouver 1998, High energy physics, vol. 2**, 1802-1808. hep-lat/9812011;
P. Chen et al., Nucl. Phys. Proc. Suppl. **73** 204, 207, 405 (1999)
- [9] S. Aoki, T. Izubuchi, Y. Kuramashi, and Y. Taniguchi, Nucl. Phys. Proc. Suppl. **83-84** 624 (2000);
S. Aoki, T. Izubuchi, Y. Kuramashi, and Y. Taniguchi, hep-lat/0004003.
- [10] G. R. Fleming, Nucl. Phys. Proc. Suppl. **83-84** 363 (2000).
- [11] P. M. Vranas, hep-lat/0001006.

- [12] CP-PACS collaboration (A. Ali Khan et al.), hep-lat/0007014.
- [13] RBC collaboration (T. Blum et. al.), hep-lat/0007038.
- [14] V. Gadiyak, X. Ji, C. Jung, hep-lat/0002023, to appear in Phys. Rev. D.
- [15] M. Atiyah and I. M. Singer, Ann. Math. **93**, 139 (1971).
- [16] R. Narayanan and H. Neuberger, Phys. Lett. B **302**, 62 (1993);
R. Narayanan and H. Neuberger, Nucl. Phys. **B412**, 574 (1994);
R. Narayanan and H. Neuberger, Phys. Rev. Lett. **71**, 3251 (1993);
R. Narayanan and H. Neuberger, Nucl. Phys. **B443**, 305 (1995).
- [17] R.G. Edwards, U. M. Heller and R. Narayanan, Nucl. Phys. **B522**, 285 (1998).
- [18] R.G. Edwards, U. M. Heller and R. Narayanan, Nucl. Phys. **B535**, 403 (1998).
- [19] M. Lüscher and P. Weisz, Phys. Lett. B **158**, 250(1985).
- [20] Y. Iwasaki, Nucl. Phys. **B258**, 141 (1985).
- [21] R.G. Edwards, U. M. Heller and R. Narayanan, Phys. Rev. D **60**, 034502 (1999).